# Improved Detection Performance for Passive Radars Exploiting Known Communication Signal Form

Anantha K. Karthik, *Student Member, IEEE*, and Rick S. Blum, *Fellow, IEEE*

***Abstract*—In this letter, we address the problem of target detection in passive multiple-input multiple-output radar networks. A generalized likelihood ratio test is derived, assuming prior knowledge of the signal format used in the noncooperative transmit stations. The performance of the generalized likelihood ratio test in the known signal format case is often significantly more favorable when compared to the case that does not exploit this information. Further, the performance improves with increasing number of samples per symbol and for a sufficiently large number of samples per symbol, the performance closely approximates that of an active radar with a known transmitted signal.**

***Index Terms*—Code-division multiple access, digital video broadcasting terrestrial standard, generalized likelihood ratio test, passive radar.**

## I. Introduction

Passive radar differs from conventional active radar in that it relies on preexisting signals from noncooperative transmitters instead of transmitting a known signal. Examples of noncooperative transmitters include radio transmitters, TV transmitters, cellular base stations, and other such high-power transmitters. Such a system is cost efficient, covert, and suitable for emergencies due to the lack of a transmitter. Consider a scenario where the passive radar system utilizes the signals transmitted from a cellular base station for target detection. Although we do not control the base station, we usually have prior information regarding the position of the transmitter along with the signal format of the transmitted signal used in the base station. The transmitted signal, however, still contains unknown information bits, so the signal is not fully known. Prior publications available in the literature derived explicit closed-form expressions for the generalized likelihood ratio tests (GLRTs) for target detection in passive multiple-input multiple-output radar (PMR) networks [1]–[8]. However, they did not consider the possibility of exploiting the available signal format information.

In [1]–[4], the discrete-time samples of the transmitted signal are assumed to be a deterministic unknown parameter. The transmitted signal along with other unknown parameters is estimated in the GLRT procedure. In [5]–[9], GLRTs were derived for target detection in scenarios where the unknown transmitted signal is modeled as stochastic. A circular Gaussian random process with zero mean and unit variance is used to model the transmitted signal. In [10], the unknown transmitted signal was modeled as an autoregressive process whose temporal correlation is estimated using the expectation maximization algorithm and is exploited for target detection.

In this letter, we study the problem of target detection in PMR networks assuming prior knowledge of the signal format of the transmitted signal and assume it to be a deterministic unknown parameter. We consider scenarios in which the transmitted signal uses either a linear digital modulation with a known pulse shape or the orthogonal frequency division multiplexing (OFDM) modulation scheme. The linear modulation scheme is used in technologies such as wide-band code division multiple access [11] and digital video broadcasting-satellite [12], whereas technologies such as digital video broadcasting-terrestrial [13], WiMAX and long-term evaluation [14] incorporate the OFDM modulation scheme.

Under the stated assumptions, we derive explicit closed-form expressions for a useful relaxed version of the GLRT for target detection in PMR networks depending on whether the noise variance is known or unknown. Numerical results show that the derived GLRTs perform significantly better than GLRTs that do not use the signal format information. Further, we observed the performance improves with the number of samples per symbol, and for a sufficiently large number of samples per symbol, the performance closely approximates that of an active radar where the transmitted signal is entirely known. Finally, the relaxation causes little loss at reasonable signal-to-noise ratios.

*Notations*: We use bold upper case, bold lower case, and italic lettering to, respectively, denote matrices, column vectors, and scalars. Notations $(.)^T$, $(.)^H$, and $\otimes$ are the transpose, Hermitian, and Kronecker product, respectively. $\boldsymbol{I}_N$ stands for a $N$-dimensional identity matrix, $\mathbf{0}_{N\times 1}$ denotes a column vector of length $N$ with all the elements equal to 0, $||.||$ is the Frobenius norm, $\mathcal{CN}(\boldsymbol{\mu}_N, \Sigma)$ denotes a $N$-dimensional complex multivariate Gaussian distribution with mean $\boldsymbol{\mu}_N$ and covariance matrix $\Sigma$, $\mathbb{C}$ denotes the set of complex numbers, and $\mathbb{R}^+$ denotes the set of positive real numbers.

## II. Signal Model and Problem Statement

We adopt the accepted model for PMR networks presented in [1]. We assume $N_t$ transmit stations, $N_r$ receive stations, and orthogonal (or separable) signals sent from each transmit station. The observations received directly from the transmitters are called reference channel signals, whereas those received from

Manuscript received July 25, 2018; revised September 9, 2018; accepted September 9, 2018. Date of publication September 14, 2018; date of current version September 20, 2018. This work was supported in part by the U.S. Army Research Laboratory and the U.S. Army Research Office under Grant W911NF-17-1-0331 and in part by the National Science Foundation under Grant ECCS-1405579 and Grant CNS-1702555. The associate editor coordinating the review of this manuscript and approving it for publication was Prof. Deanna Needell.
*(Corresponding author: Anantha K. Karthik.)*

The authors are with the Department of Electrical and Computer Engineering, Lehigh University, Bethlehem, PA 18015 USA (e-mail: akk314@lehigh.edu; rblum@lehigh.edu).

Color versions of one or more of the figures in this letter are available online at http://ieeexplore.ieee.org.

Digital Object Identifier 10.1109/LSP.2018.2870341

the possible reflection from the target are called surveillance channel signals. The reference and surveillance channel signals are separated using beamforming. After isolating the signals, each channel contains a certain amount of noise/clutter in addition to a scaled, delayed, and Doppler-shifted version of the transmitted signal. As in [1], we assume delay-Doppler compensation accounts for the time delay and frequency shifts on the originally transmitted signal since we are testing for a target with a known position and Doppler. As in [1], we assume the noise/clutter has been whitened.

Let $\boldsymbol{s}_s^{ij} \in \mathbb{C}^{N\times 1}$ and $\boldsymbol{s}_r^{ij} \in \mathbb{C}^{N\times 1}$ denote the surveillance and reference channel signals, respectively, between the $i$th transmit station and $j$th receive station. The PMR detection problem involves discriminating between the presence or absence of a target within a hypothesized Cartesian position-velocity cell under test [1]. The problem can be formulated as a binary hypothesis test between the target-absent hypothesis ($\mathcal{H}_0$), and the target-present hypothesis ($\mathcal{H}_1$) as

$$\begin{aligned} \mathcal{H}_0 : \boldsymbol{s}_s^{ij} &= \boldsymbol{n}_s^{ij} \\ \boldsymbol{s}_r^{ij} &= \mu_r^{ij}\boldsymbol{u}^i + \boldsymbol{n}_r^{ij} \\ \mathcal{H}_1 : \boldsymbol{s}_s^{ij} &= \mu_s^{ij}\boldsymbol{u}^i + \boldsymbol{n}_s^{ij} \\ \boldsymbol{s}_r^{ij} &= \mu_r^{ij}\boldsymbol{u}^i + \boldsymbol{n}_r^{ij} \end{aligned} \tag{1}$$

for $i = 1, 2, \ldots, N_t$ and $j = 1, 2, \ldots, N_r$. In (1), $\mu_s^{ij}$ and $\mu_r^{ij}$ are the unknown complex surveillance and reference channel coefficients, respectively, that include any gain due to beamforming and the noise vectors $\boldsymbol{n}_r^{ij}$ and $\boldsymbol{n}_s^{ij}$ are circular Gaussian noise, distributed as $\mathcal{CN}(\boldsymbol{0}_{N\times 1}, \sigma^2 \boldsymbol{I}_N)$ with $\sigma^2$ denoting the noise variance. Further, $\boldsymbol{u}^i \in \mathbb{C}^{N\times 1}$ contains samples of the unknown transmitted signal from the $i$th transmit station. In this letter, we only consider scenarios in which the transmitted signal vector $\boldsymbol{u}_i$ can be expressed as

$$\boldsymbol{u}^i = \boldsymbol{G}^i \boldsymbol{b}^i. \tag{2}$$

In (2), $\boldsymbol{G}^i$ is a known matrix of appropriate size and $\boldsymbol{b}^i$ is a column vector of appropriate size containing unknown complex symbols from a digital modulation scheme.

A number of communication signals including linear digital modulations and OFDM signals can be expressed in the form shown in (2).[1] For example, consider an OFDM signal. The complex baseband structure of an OFDM signal can be represented as [13]

$$u^i(t + nT_{\text{sym}}) = \sum_{l=0}^{N_s-1} e^{j2\pi \frac{l}{T_{\text{u}}}(t-T_{\text{g}})} b_{nl}^i \tag{3}$$

for $0 \le t < T_{\text{sym}}$. In (3), $i$ denotes the index of the transmit station, $n$ denotes the OFDM symbol number, $N_s$ is the number of subcarriers used in the OFDM signal, $b_{nl}^i$ is a complex valued modulation symbol, $T_u$ is the duration of the useful part of the OFDM symbol (excluding the guard interval), $T_g$ is the guard interval duration, and $T_{\text{sym}} = (T_u + T_g)$ is the total OFDM symbol duration. Let $T_s$ be the sampling rate equal to $T_{\text{sym}}/(N_s P)$, where $P$ is the number of samples per complex symbol. Collecting $N = LN_sP$ samples from $L$ consecutive OFDM symbols indexed by $0, 1, \ldots, (L-1)$, the transmitted signal samples can be expressed as

$$\boldsymbol{u}^i = (\boldsymbol{I}_L \otimes \boldsymbol{H})\boldsymbol{b}^i \tag{4}$$

where $\boldsymbol{u}^i = [(\boldsymbol{u}_0^i)^T, (\boldsymbol{u}_1^i)^T, \ldots, (\boldsymbol{u}_{L-1}^i)^T]^T$ with $\boldsymbol{u}_k^i = [u^i(kT_{\text{sym}}), u^i(T_s + kT_{\text{sym}}), \ldots, u^i((N_sP-1)T_s + kT_{\text{sym}})]^T$ for $k = 0, 1, \ldots, L-1$, and $\boldsymbol{b}^i = [(\boldsymbol{b}_0^i)^T, (\boldsymbol{b}_1^i)^T, \ldots, (\boldsymbol{b}_{L-1}^i)^T]^T$ with $\boldsymbol{b}_k^i = [b_{k0}^i, b_{k1}^i, \ldots, b_{k(N_s-1)}^i]^T$ for $k = 0, 1, \ldots, L-1$. In (4), $\boldsymbol{H}$ is a $N_sP \times N_s$ matrix whose $ml$th element is given by $h_{ml} = e^{\frac{j2\pi l(mT_s - T_g)}{T_u}}$ for $m = 0, 1, \ldots, N_sP-1$ and $l = 0, 1, \ldots, N_s - 1$. In this letter, we derive a relaxed GLRT for target detection in PMR networks that uses the available information regarding the signal format of the transmitted signal.

## III. Target Detection in PMR Networks

Define $\boldsymbol{s}_s^i = [(\boldsymbol{s}_s^{i1})^T, \ldots, (\boldsymbol{s}_s^{iN_r})^T]^T$, $\boldsymbol{s}_r^i = [(\boldsymbol{s}_r^{i1})^T, \ldots, (\boldsymbol{s}_r^{iN_r})^T]^T$ and $\boldsymbol{s}^i = [(\boldsymbol{s}_s^i)^T, (\boldsymbol{s}_r^i)^T]^T$ for $i = 1, 2, \ldots, N_t$. Similarly, define $\boldsymbol{\mu}_s^i = [\mu_s^{i1}, \ldots, \mu_s^{iN_r}]^T$ and $\boldsymbol{\mu}_r^i = [\mu_r^{i1}, \ldots, \mu_r^{iN_r}]^T$ for $i = 1, 2, \ldots, N_t$. Let $\boldsymbol{s} = \left[(\boldsymbol{s}^1)^T, \ldots, (\boldsymbol{s}^{N_t})^T\right]^T$, $\boldsymbol{\mu}_s = [(\boldsymbol{\mu}_s^1)^T, \ldots, (\boldsymbol{\mu}_s^{N_t})^T]^T$, and $\boldsymbol{\mu}_r = [(\boldsymbol{\mu}_r^1)^T, \ldots, (\boldsymbol{\mu}_r^{N_t})^T]^T$. Finally, let $\boldsymbol{u} = [(\boldsymbol{u}^1)^T, \ldots, (\boldsymbol{u}^{N_t})^T]^T$ with $\boldsymbol{u}^i$ from (2).

The received signals $\boldsymbol{s}_r^{ij}$ and $\boldsymbol{s}_s^{ij}$ are parameterized by $\mu_r^{ij}$, $\mu_s^{ij}$, and $\boldsymbol{b}^i$. Since these parameters are unknown to the PMR system, we employ the GLRT for the hypotheses testing problem given in (1). In GLRTs, we replace the unknown deterministic quantities with the corresponding maximum likelihood estimates (MLE). However, obtaining the MLE of the constellation symbols $b_k^i$ might not be tractable as we would have to search across all possible sequences of $\boldsymbol{b}^i$. Hence, we introduce a relaxation, called the relaxed GLRT, where we allow $b_k^i$ to be any complex number, i.e., $b_k^i \in \mathbb{C}$ as opposed to an actual modulation symbol from the defined finite set. Under this assumption, let $\boldsymbol{b}^i \in \mathbb{C}^{\mathcal{B}_i \times 1}$ and $\boldsymbol{b} = \left[(\boldsymbol{b}^1)^T, \ldots, (\boldsymbol{b}^{N_t})^T\right]^T \in \mathbb{C}^{\mathcal{B}\times 1}$ with $\mathcal{B} = \sum_{i=1}^{N_t} \mathcal{B}_i$.

### A. Relaxed GLRT for PMR Networks When the Signal Format Information is Employed and $\sigma^2$ is Known

The conditional probability density function (pdf) of $\boldsymbol{s}$ under $\mathcal{H}_1$ is given by $p_1(\boldsymbol{s}|\boldsymbol{\mu}_s, \boldsymbol{\mu}_r, \boldsymbol{b}) = \prod_{i=1}^{N_t} p_1^i(\boldsymbol{s}^i|\boldsymbol{\mu}_s^i, \boldsymbol{\mu}_r^i, \boldsymbol{b}^i)$, where $p_1^i(\boldsymbol{s}^i|\boldsymbol{\mu}_s^i, \boldsymbol{\mu}_r^i, \boldsymbol{b}^i) \propto \exp\{\frac{-1}{\sigma^2}\sum_{j=1}^{N_r}(||\boldsymbol{s}_s^{ij} - \mu_s^{ij}\boldsymbol{G}^i\boldsymbol{b}^i||^2 + ||\boldsymbol{s}_r^{ij} - \mu_r^{ij}\boldsymbol{G}^i\boldsymbol{b}^i||^2)\}$. Similarly, the conditional pdf of $\boldsymbol{s}$ under $\mathcal{H}_0$ is given by $p_0(\boldsymbol{s}|\boldsymbol{\mu}_r, \boldsymbol{b}) = \prod_{i=1}^{N_t} p_0^i(\boldsymbol{s}^i|\boldsymbol{\mu}_r^i, \boldsymbol{b}^i)$, where $p_0^i(\boldsymbol{s}^i|\boldsymbol{\mu}_r^i, \boldsymbol{b}^i) \propto \exp\{\frac{-1}{\sigma^2}\sum_{j=1}^{N_r}||\boldsymbol{s}_r^{ij} - \mu_r^{ij}\boldsymbol{G}^i\boldsymbol{b}^i||^2\}$. Let $l_1(\boldsymbol{\mu}_s, \boldsymbol{\mu}_r, \boldsymbol{b}|\boldsymbol{s}) = \log p_1(\boldsymbol{s}|\boldsymbol{\mu}_s, \boldsymbol{\mu}_r, \boldsymbol{b})$ and $l_0(\boldsymbol{\mu}_r, \boldsymbol{b}|\boldsymbol{s}) = \log p_0(\boldsymbol{s}|\boldsymbol{\mu}_r, \boldsymbol{b})$ denote the log-likelihood functions under the hypotheses $\mathcal{H}_1$ and $\mathcal{H}_0$. The relaxed GLRT can now be written as

$$\max_{\{\boldsymbol{\mu}_s, \boldsymbol{\mu}_r, \boldsymbol{b}\} \in \mathbb{C}^{N_rN_t} \times \mathbb{C}^{N_rN_t} \times \mathbb{C}^{\mathcal{B}}} l_1(\boldsymbol{\mu}_s, \boldsymbol{\mu}_r, \boldsymbol{b}|\boldsymbol{s}) - \max_{\{\boldsymbol{\mu}_r, \boldsymbol{b}\} \in \mathbb{C}^{N_rN_t} \times \mathbb{C}^{\mathcal{B}}} l_0(\boldsymbol{\mu}_r, \boldsymbol{b}|\boldsymbol{s}) \underset{\mathcal{H}_0}{\overset{\mathcal{H}_1}{\gtrless}} \kappa_{ksf} \tag{5}$$

where $\kappa_{ksf}$ denotes a threshold corresponding to a desired value of false alarm probability. It is shown in Appendix that the GLRT-based target detector in (5), termed the *PMR Relaxed*

[1] See [15] for examples of OFDM and linear digital modulation schemes that can be expressed in the form shown in (2).

**Algorithm 1:** Target Detection Algorithm for PMR Networks using Signal Information

**if** $\sigma^2$ *is known* **then**
  Determine the threshold $\kappa_{ksf}$ according to the desired false alarm probability;
  Use (6) to determine if the target is present or not.
**else**
  Determine the threshold $\kappa_{uk}$ according to the desired false alarm probability;
  Use (7) to determine if the target is present or not.
**end**

*GLRT with Known signal format and known noise variance (PMR-RGLRT-K)*, is given by

$$\xi_{ksf} = \frac{1}{\sigma^2}\sum_{i=1}^{N_t}\Big[\lambda_1\left((\boldsymbol{G}^i)^H\boldsymbol{\phi}_1^i(\boldsymbol{\phi}_1^i)^H\boldsymbol{G}^i,(\boldsymbol{G}^i)^H\boldsymbol{G}^i\right) - \lambda_1\left((\boldsymbol{G}^i)^H\boldsymbol{\phi}_r^i(\boldsymbol{\phi}_r^i)^H\boldsymbol{G}^i,(\boldsymbol{G}^i)^H\boldsymbol{G}^i\right)\Big] \underset{\mathcal{H}_0}{\overset{\mathcal{H}_1}{\gtrless}} \kappa_{ksf} \quad (6)$$

where $\lambda_1(\mathbf{A},\mathbf{B})$ denotes the largest generalized eigenvalue of the generalized eigenvalue problem $\boldsymbol{A}\boldsymbol{w} = \lambda\boldsymbol{B}\boldsymbol{w}$ and $\boldsymbol{\phi}_1^i = [\boldsymbol{\phi}_s^i, \boldsymbol{\phi}_r^i]$ with $\boldsymbol{\phi}_s^i = \left[\boldsymbol{s}_s^{i1}, \boldsymbol{s}_s^{i2}, \ldots, \boldsymbol{s}_s^{iN_r}\right]$ and $\boldsymbol{\phi}_r^i = \left[\boldsymbol{s}_r^{i1}, \boldsymbol{s}_r^{i2}, \ldots, \boldsymbol{s}_r^{iN_r}\right]$.

When $\sigma^2$ is unknown, following similar steps as in Appendix, the GLRT-based target detector, termed the *PMR Relaxed GLRT with Unknown noise variance and Known signal format (PMR-RGLRT-UK)*, is given by

$$\frac{\sum_{i=1}^{N_t} E_{sr}^i - \lambda_1\left((\boldsymbol{G}^i)^H\boldsymbol{\phi}_r^i(\boldsymbol{\phi}_r^i)^H\boldsymbol{G}^i,(\boldsymbol{G}^i)^H\boldsymbol{G}^i\right)}{\sum_{i=1}^{N_t} E_{sr}^i - \lambda_1\left((\boldsymbol{G}^i)^H\boldsymbol{\phi}_1^i(\boldsymbol{\phi}_1^i)^H\boldsymbol{G}^i,(\boldsymbol{G}^i)^H\boldsymbol{G}^i\right)} \underset{\mathcal{H}_0}{\overset{\mathcal{H}_1}{\gtrless}} \kappa_{uk} \quad (7)$$

where $\kappa_{uk}$ denotes a threshold corresponding to a desired value of false alarm probability and $E_{sr}^i = ||\boldsymbol{s}_s^i||^2 + ||\boldsymbol{s}_r^i||^2$. See [15] for full derivation in this scenario. The target detection algorithms for both the considered scenarios are presented in Algorithm 1.

## IV. Simulation Results

In this section, we compare the performance of the proposed GLRT-based target detectors to other GLRT-based detectors available in the literature via numerical simulations. We consider the active (known signal) multiple-input multiple-output radar GLRT proposed in [16] and the PMR GLRT without using the signal format information (PMR-GLRT) proposed in [1].

### A. Simulation Scenario

For a fair comparison, we follow the simulation setup of [1]. We consider a PMR network with $N_t = 2$ transmit stations and $N_r = 3$ receive stations. Following [1], we fix $||\boldsymbol{u}^i||^2 = N$. The transmitted signal samples $\boldsymbol{u}^i$ are generated according to the chosen signal format in (2) across all transmit stations. As in [1], the reference channel coefficients $\boldsymbol{\mu}_r^i$ are randomly drawn from a $\mathcal{CN}(\mathbf{0}_{N_r}, \boldsymbol{I}_{N_r})$ distribution on each trial under $\mathcal{H}_0$ and $\mathcal{H}_1$, and then scaled to achieve a desired direct-path signal-to-noise ratio ($\text{DNR}_{\text{avg}}^i$) according to $\text{DNR}_{\text{avg}}^i = \frac{||\boldsymbol{\mu}_r^i||^2}{N_r\sigma^2}$ on each trial, where $\boldsymbol{\mu}_r^i = [\mu_r^{i1}, \ldots, \mu_r^{iN_r}]^T$ and $|\mu_r^{ij}|^2/\sigma^2$ is the DNR of the $ij$th reference channel. Surveillance channel coefficients are similarly drawn from a $\mathcal{CN}(\mathbf{0}_{N_r}, \boldsymbol{I}_{N_r})$ distribution and scaled to achieve a desired surveillance signal-to-noise ratio ($\text{SNR}_{\text{avg}}^i$) according to $\text{SNR}_{\text{avg}}^i = \frac{||\boldsymbol{\mu}_s^i||^2}{N_r\sigma^2}$ on each trial, where $\boldsymbol{\mu}_r^i = [\mu_r^{i1}, \ldots, \mu_r^{iN_r}]^T$ and $|\mu_s^{ij}|^2/\sigma^2$ is the SNR of the $ij$th surveillance channel. For simplicity, we assume that $\text{SNR}_{\text{avg}}^i = \text{SNR}_{\text{avg}}$ for all $i$, i.e., the average surveillance channel target-path SNR across receivers is the same for each transmit channel. Similarly, we assume $\text{DNR}_{\text{avg}}^i = \text{DNR}_{\text{avg}}$ and $\boldsymbol{G}^i(.) = \boldsymbol{G}(.)$ for all $i$.

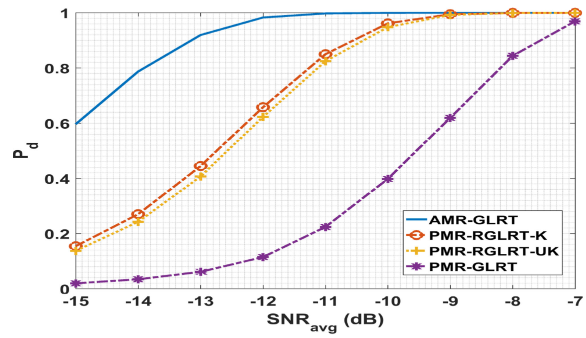


(a)

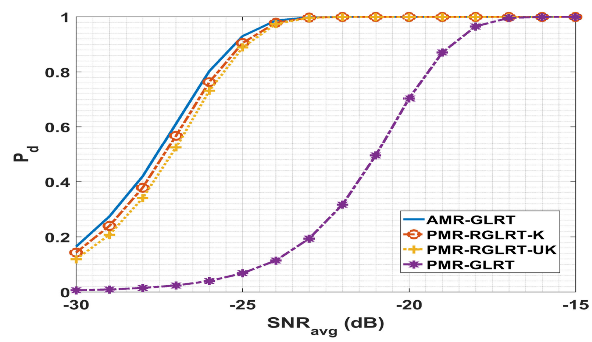


(b)

Fig. 1. $P_d$ curves as a function of $\text{SNR}_{\text{avg}}$ when the transmitted signal is an OFDM signal with $N_s = 16$ subcarriers and $\text{DNR}_{\text{avg}} = -10$ dB for different values of samples per symbol $P$. (a) $P = 4$. (b) $P = 64$.

In our simulations, we consider the case where the transmitted signal follows the OFDM modulation scheme. The signal is generated according to (3). The guard interval duration $T_g$ is set to 0 $\mu$s and BPSK symbols are modulated on each subcarrier of the OFDM symbol.[2] We use 1 OFDM symbol for target detection in all the considered cases. The BPSK symbols used in the generation of the transmitted signal are randomly generated for each Monte Carlo simulation run. For the considered target detectors, the detection threshold that achieves a probability of false alarm ($P_f$) of $10^{-3}$ is determined empirically using $10^5$ trials under $\mathcal{H}_0$, and the probability of detection ($P_d$) is estimated using $10^4$ trials under $\mathcal{H}_1$.

### B. Numerical Results

*1) Dependence on $\text{SNR}_{avg}$, $\text{DNR}_{avg}$, and $P$:* Fig. 1 shows the $P_d$ curves as a function of $\text{SNR}_{\text{avg}}$ for $\text{DNR}_{\text{avg}} = -10$ dB and for different values of samples per symbol, $P$. The number of subcarriers in the OFDM symbol is fixed to 16 (total of

[2] In this letter, we consider the target detection model presented in [1]. In this model, all the channels are flat fading channels, so there is no multipath in the considered scenario. Hence, there would no need of a guard interval as there is no intersymbol interference. So we set $T_g$ to 0 for ease of simulation.

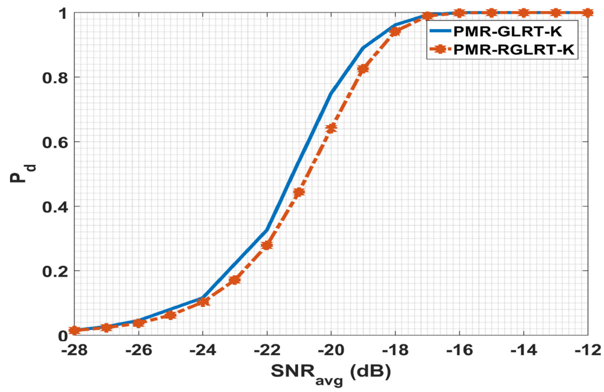


Fig. 2. $P_d$ curves as a function of $\text{SNR}_{\text{avg}}$ when the transmitted signal is an OFDM signal with $N_s = 16$ subcarriers and $\text{DNR}_{\text{avg}} = -10$ dB for samples per symbol $P = 16$.

$16P$ samples). As we can see from the numerical results, the proposed target detectors significantly outperform the GLRT-based target detectors that do not use the available signal format information. The detection performance of relaxed GLRT-based target detectors improves significantly with increasing $P$ when compared to *PMR-GLRT*.[3] This performance gain is primarily due to the lower number of parameters that need to be estimated for the GLRT in the known signal format case. For a sufficiently large value of $P$, we can also see that the performance of the proposed target detectors is close to that of an active radar, which has complete knowledge of the transmitted signal. Finally, we observe no significant loss in the detection performance from not knowing noise variance in the proposed target detectors for all the considered cases.

*2) Performance Comparison With Unrelaxed GLRT:* In this letter, we introduced a relaxation on the complex symbols $\boldsymbol{b}^i$ to make the search for the MLE tractable. We now compare the performance of the relaxed GLRT to the exact unrelaxed GLRT to study the performance loss caused by using the relaxation. The exact GLRT that uses the signal format information is obtained by searching across all possible sequences of $\boldsymbol{b}^i$ and finding the sequence that maximizes the likelihood. The *PMR GLRT using the signal format information* (*PMR-GLRT-K*) is given by

$$\max_{\{\boldsymbol{\mu}_s,\boldsymbol{\mu}_r,\boldsymbol{b}\}\in\mathbb{C}^{N_rN_t}\times\mathbb{C}^{N_rN_t}\times\mathbb{A}^{\mathcal{B}}} l_1(\boldsymbol{\mu}_s,\boldsymbol{\mu}_r,\boldsymbol{b}|\boldsymbol{s}) - \max_{\{\boldsymbol{\mu}_r,\boldsymbol{b}\}\in\mathbb{C}^{N_rN_t}\times\mathbb{A}^{\mathcal{B}}} l_0(\boldsymbol{\mu}_r,\boldsymbol{b}|\boldsymbol{s}) \underset{\mathcal{H}_0}{\overset{\mathcal{H}_1}{\gtrless}} \kappa_{\text{pmrk}} \tag{8}$$

where $\kappa_{\text{pmrk}}$ denotes a threshold corresponding to a desired false alarm probability and $\mathbb{A}$ is the finite set of complex symbols from which the complex symbols $\boldsymbol{b}^i$ are taken.

For this comparison, the number of subcarriers in the OFDM symbol fixed to 16 (total of $16P$ samples). The direct-path signal-to-noise ratio, $\text{DNR}_{\text{avg}}$, is fixed to $-10$ dB and detection threshold corresponds to a $P_f$ of $10^{-3}$. Since $\boldsymbol{b}^i \in \mathbb{A}^{16}$, we search across all $2^{16}$ possible sequences to get the MLE of $\boldsymbol{b}^i$. Fig. 2 shows us the performance loss of using the relaxation for $P = 16$. We can see from the results that the performance loss in the target detection due to the relaxation is relatively small.

[3]The target detection performance of *PMR-GLRT* improves with increasing number of samples. However, it improves at a much slower rate when compared to the proposed relaxed GLRT-based target detectors.

## V. Conclusion

This letter presented a GLRT-based passive radar target detectors that can use the available signal format information under conditions where either the noise variance is known or unknown. As demonstrated, adding additional known information about the transmitted signal into the GLRT improves performance in comparison to a GLRT where the information is not utilized, and the signal is considered entirely unknown. Further, given an adequate number of samples per symbol, the proposed target detectors may be used to close the performance gap between the passive and active radar.

## Appendix
## Derivation of PMR-RGLRT-K When the Signal Format Information is Employed

Consider hypothesis $\mathcal{H}_1$ in (1). We have

$$l_1(\boldsymbol{\mu}_s,\boldsymbol{\mu}_r,\boldsymbol{b}|\boldsymbol{s}) = \sum_{i=1}^{N_t} l_1^i(\boldsymbol{\mu}_s^i,\boldsymbol{\mu}_r^i,\boldsymbol{b}^i|\boldsymbol{s}^i) \tag{9}$$

where (ignoring the additive constants) we have $l_1^i(\boldsymbol{\mu}_s^i,\boldsymbol{\mu}_r^i,\boldsymbol{b}^i|\boldsymbol{s}^i) = -\frac{\sum_{j=1}^{N_r}\left(||\boldsymbol{s}_s^{ij}-\mu_s^{ij}\boldsymbol{G}^i\boldsymbol{b}^i||^2+||\boldsymbol{s}_r^{ij}-\mu_r^{ij}\boldsymbol{G}^i\boldsymbol{b}^i||^2\right)}{\sigma^2}$. The MLE of $\mu_s^{ij}$ and $\mu_r^{ij}$ obtained from setting the derivative of (9) with respect to $\mu_s^{ij}$ and $\mu_r^{ij}$ to zero are given by

$$\hat{\mu}_s^{ij} = \frac{(\boldsymbol{G}^i\boldsymbol{b}^i)^H\boldsymbol{s}_s^{ij}}{(\boldsymbol{G}^i\boldsymbol{b}^i)^H\boldsymbol{G}^i\boldsymbol{b}^i} \text{ and } \hat{\mu}_r^{ij} = \frac{(\boldsymbol{G}^i\boldsymbol{b}^i)^H\boldsymbol{s}_r^{ij}}{(\boldsymbol{G}^i\boldsymbol{b}^i)^H\boldsymbol{G}^i\boldsymbol{b}^i}. \tag{10}$$

Substituting $\hat{\mu}_s^{ij}$ and $\hat{\mu}_r^{ij}$ in $l_1^i(\boldsymbol{\mu}_s^i,\boldsymbol{\mu}_r^i,\boldsymbol{b}^i|\boldsymbol{s}^i)$ and simplifying, we obtain

$$l_1^i(\hat{\boldsymbol{\mu}}_s^i,\hat{\boldsymbol{\mu}}_r^i,\boldsymbol{b}^i|\boldsymbol{s}^i) = \frac{-1}{\sigma^2}\left[E_{sr}^i - \frac{(\boldsymbol{G}^i\boldsymbol{b}^i)^H\boldsymbol{\phi}_1^i(\boldsymbol{\phi}_1^i)^H\boldsymbol{G}^i\boldsymbol{b}^i}{(\boldsymbol{G}^i\boldsymbol{b}^i)^H\boldsymbol{G}^i\boldsymbol{b}^i}\right]. \tag{11}$$

The value of $\boldsymbol{b}^i$ that maximizes (11) is given by $\hat{\boldsymbol{b}}^i = \boldsymbol{v}_1\left((\boldsymbol{G}^i)^H\boldsymbol{\phi}_1^i(\boldsymbol{\phi}_1^i)^H\boldsymbol{G}^i,(\boldsymbol{G}^i)^H\boldsymbol{G}^i\right)$, where $\boldsymbol{v}_1(\mathbf{A},\mathbf{B})$ denotes the generalized eigenvector corresponding to the maximum generalized eigenvalue. Substituting $\hat{\boldsymbol{b}}^i$ in (11) and simplifying (9), we have

$$l_1(\hat{\boldsymbol{\mu}}_s,\hat{\boldsymbol{\mu}}_r,\hat{\boldsymbol{b}}|\boldsymbol{s}) = \frac{-\sum_{i=1}^{N_t}\left(E_{sr}^i - \lambda_1\left((\boldsymbol{G}^i)^H\boldsymbol{\phi}_1^i(\boldsymbol{\phi}_1^i)^H\boldsymbol{G}^i,(\boldsymbol{G}^i)^H\boldsymbol{G}^i\right)\right)}{\sigma^2}.$$

Following a similar procedure, it can be shown under $\mathcal{H}_0$ that

$$l_0(\hat{\boldsymbol{\mu}}_r,\hat{\boldsymbol{b}}|\boldsymbol{s}) = \frac{-\sum_{i=1}^{N_t}\left(E_{sr}^i - \lambda_1\left((\boldsymbol{G}^i)^H\boldsymbol{\phi}_r^i(\boldsymbol{\phi}_r^i)^H\boldsymbol{G}^i,(\boldsymbol{G}^i)^H\boldsymbol{G}^i\right)\right)}{\sigma^2}.$$

Using $l_1(\hat{\boldsymbol{\mu}}_s,\hat{\boldsymbol{\mu}}_r,\hat{\boldsymbol{b}}|\boldsymbol{s})$ and $l_0(\hat{\boldsymbol{\mu}}_r,\hat{\boldsymbol{b}}|\boldsymbol{s})$, the *PMR-RGLRT-K* is given by

$$\xi_{ksf} = \frac{1}{\sigma^2}\sum_{i=1}^{N_t}\Big[\lambda_1\left((\boldsymbol{G}^i)^H\boldsymbol{\phi}_1^i(\boldsymbol{\phi}_1^i)^H\boldsymbol{G}^i,(\boldsymbol{G}^i)^H\boldsymbol{G}^i\right) - \lambda_1\left((\boldsymbol{G}^i)^H\boldsymbol{\phi}_r^i(\boldsymbol{\phi}_r^i)^H\boldsymbol{G}^i,(\boldsymbol{G}^i)^H\boldsymbol{G}^i\right)\Big] \underset{\mathcal{H}_0}{\overset{\mathcal{H}_1}{\gtrless}} \kappa_{ksf}. \tag{12}$$

## REFERENCES

[1] D. E. Hack, L. K. Patton, B. Himed, and M. A. Saville, "Detection in passive MIMO radar networks," *IEEE Trans. Signal Process.*, vol. 62, no. 11, pp. 2999–3012, Jun. 2014.

[2] D. E. Hack, L. K. Patton, and B. Himed, "Detection in passive MIMO radar networks," in *Proc. IEEE Radar Conf.*, May 2014, pp. 780–785.

[3] D. E. Hack, L. K. Patton, B. Himed, and M. A. Saville, "Centralized passive MIMO radar detection without direct-path reference signals," *IEEE Trans. Signal Process.*, vol. 62, no. 11, pp. 3013–3023, Jun. 2014.

[4] J. Liu, H. Li, and B. Himed, "Two target detection algorithms for passive multistatic radar," *IEEE Trans. Signal Process.*, vol. 62, no. 22, pp. 5930–5939, Nov. 2014.

[5] G. Cui, J. Liu, H. Li, and B. Himed, "Target detection for passive radar with noisy reference channel," in *Proc. IEEE Radar Conf.*, May 2014, pp. 144–148.

[6] G. Cui, J. Liu, H. Li, and B. Himed, "Signal detection with noisy reference for passive sensing," *Signal Process.*, vol. 108, pp. 389–399, 2015. [Online]. Available: http://www.sciencedirect.com/science/article/pii/S0165168414004587

[7] Y. Wang, L. L. Scharf, I. Santamara, and H. Wang, "Canonical correlations for target detection in a passive radar network," in *Proc. 50th Asilomar Conf. Signals, Syst., Comput.*, Nov. 2016, pp. 1159–1163.

[8] I. Santamaria, L. L. Scharf, J. Via, H. Wang, and Y. Wang, "Passive detection of correlated subspace signals in two MIMO channels," *IEEE Trans. Signal Process.*, vol. 65, no. 20, pp. 5266–5280, Oct. 2017.

[9] X. Zhang, H. Li, and B. Himed, "Multistatic detection for passive radar with direct-path interference," *IEEE Trans. Aerosp. Electron. Syst.*, vol. 53, no. 2, pp. 915–925, Apr. 2017.

[10] X. Zhang, H. Li, and B. Himed, "Multistatic passive detection with parametric modeling of the IO waveform," *Signal Process.*, vol. 141, pp. 187–198, 2017. [Online]. Available: http://www.sciencedirect.com/science/article/pii/S016516841730213X

[11] H. Lilja and H. Mattila, "WCDMA uplink modulation scheme evolution and transmitter implementation," in *Proc. Gateway 21st Century Commun. IEEE VTS 50th Veh. Technol. Conf.*, 1999, vol. 2, pp. 899–903.

[12] S. Miller, "Digital Satellite TV Broadcasting (DVB-S)." [Online]. Available: http://www.ece.ubc.ca/ edc/7860/presentations/dvb-s.pdf

[13] J. E. Palmer, H. A. Harms, S. J. Searle, and L. Davis, "DVB-T passive radar signal processing," *IEEE Trans. Signal Process.*, vol. 61, no. 8, pp. 2116–2126, Apr. 2013.

[14] U. R. Mori, P. M. Chandarana, G. V. Gajjar, and S. Dasi, "Performance comparison of different modulation schemes in advanced technologies WiMAX and LTE," in *Proc. IEEE Int. Adv. Comput. Conf.*, Jun. 2015, pp. 286–289.

[15] A. K. Karthik and R. S. Blum, "Improved detection performance of passive radars exploiting known communication signal form," May 2018. [Online]. Available: https://arxiv.org/abs/1805.01503

[16] Q. He, N. H. Lehmann, R. S. Blum, and A. M. Haimovich, "MIMO radar moving target detection in homogeneous clutter," *IEEE Trans. Aerosp. Electron. Syst.*, vol. 46, no. 3, pp. 1290–1301, Jul. 2010.